

# The ratio of Mezzanine Distortion in Steel Buildings with a new Earthquake Damage Potential Index

—

Luis Eduardo Cornelio Gutiérrez  
142d16117@egresados.ujat.mx  
ORCID: 0000-0002-3873-7759

Sergio Alberto Díaz Alvarado  
alberto.diaz@ujat.mx  
ORCID: 0000-0003-3736-9154

René Sebastián Mora Ortiz  
rene.mora@ujat.mx  
ORCID: 0000-0001-9265-7621

Alberto Vásquez Martínez  
alberto.vasquez@ujat.mx  
ORCID: 0000-0003-4909-6501

UNIVERSIDAD JUÁREZ AUTÓNOMA DE TABASCO, CUNDUACÁN, TABASCO, MÉXICO



To quote this article:

Cornelio Gutiérrez, L. E., Díaz Alvarado, S. A., Mora Ortiz, R. S., & Vásquez Martínez, A. Relación de la distorsión de entrepiso en edificios de acero con un nuevo índice del potencial de daño de los sismos. *Espacio I+D, Innovación más Desarrollo*, 12(32). <https://doi.org/10.31644/IMASD.32.2023.a04>

— Abstract —

The expected earthquake damage in the buildings can be determined with the maximum mezzanine distortion ( $\theta_{\max}$ ) and depends on the building type and the earthquake characteristics. In this research, a new earthquake damage potential index ( $\text{DPI}_{\text{SaT1-IA-}\Delta\text{IA}}$ ) is presented based on its Arias intensity ( $I_A$ ), its significant duration ( $\Delta_{IA}$ ), and the spectral acceleration for the fundamental period of the building ( $\text{SaT1}$ ). In addition, predictive equations are developed to determine the  $\theta_{\max}$  as a function of the new index. Two 2D buildings, with 3 and 7 stories, are used, and Oaxaca City, Mexico, is considered the study area. Forty-six accelerograms of horizontal components of real strong ground motion records are used. For these accelerograms set based on a spectral matching method, accelerograms with spectral response compatible with the design spectrum of the Mexican seismic standard from the city studied are generated. The seismic response of the buildings is obtained by the incremental non-linear dynamic analysis. The results show a good correlation between  $\theta_{\max}$  with the  $\text{SA}_{T1}$  and  $I_A$  in the analyzed set of compatible accelerograms. The  $\text{DPI}_{\text{SaT1-IA-}\Delta\text{IA}}$  proposed has a better correlation with  $\theta_{\max}$  than  $\text{SA}_{T1}$  and  $I_A$ , for real and compatible accelerograms in the two buildings studied. Therefore, it can be a better alternative to measure the destructiveness potential of seismic action. Finally, the predictive equations were developed to allow the new index to correctly relate to the  $\theta_{\max}$  for compatible seismic actions in steel buildings.

**Keywords:**

*Inter-story drift; significant duration; spectral acceleration for the fundamental mode; steel frames; destructive potential of earthquakes.*

As a learning of the different seismic events that occurred in recent decades, it has been demonstrated that the damage that occurs in buildings during these events is related to the lateral displacements that occur on the floors of the buildings (Barbat *et al.*, 2010; Kostinakis *et al.*, 2014; Perrault & Guéguen, 2015). To ensure proper behavior of buildings in the face of seismic actions, current regulations in the world, such as ASCE 7-16 in the United States (ASCE/SEI 7-16, 2016), the Civil Works Design Manual of the Federal Electricity Commission of Mexico (MDOC-CFE, 2015), Eurocode 8 (CEN, 2019), establish the lateral displacements allowed for the different structural systems. This is done by limiting the maximum difference between the lateral displacements of consecutive floors produced by seismic forces, divided by the mezzanine's height; this value is called "maximum mezzanine distortion" ( $\theta_{\max}$ ). For the  $\theta_{\max}$  estimated in a seismic evaluation to be adequate, it is vital to make a correct definition of the seismic threat of the study area. In the field of seismic engineering, the two most accepted ways to characterize the seismic threat of a site are accelerograms and response spectra. Accelerograms are temporary records of the site at ground acceleration values measured in two orthogonal horizontal directions (North-South [N-S] and East-West [E-W] component) and one vertical occurring during the seismic event. The use of accelerograms in a non-linear dynamic analysis (ADNL) of a building in its incremental dynamic analysis (IDA) mode (Vamvatsikos & Cornell, 2002) allows estimating the temporal evolution of the maximum response of the structure in terms of forces, displacements, etc., depending on the increased variable that, generally, is the intensity of the seismic action. In this way, the possible expected consequences (damage) in the buildings are adequately obtained (Díaz *et al.*, 2018; Kazantzi *et al.*, 2014; Vamvatsikos, 2014; Vargas *et al.*, 2018). On the other hand, the respective "acceleration response spectrum (Sa)" can be obtained through the accelerograms; the same that represents the expected maximum of soil acceleration and the respective spectral accelerations for different structural periods (Newmark & Hall, 1982). In the seismic regulations in a simplified way, the seismic threat is characterized based on the so-called "design spectra (Sa design)"; obtained as an envelope of the seismic response spectra of a site or as a result of a seismic hazard study, where the influence of all possible seismic sources, their historical seismicity (or frequency with which earthquakes occur) and their intensity are contemplated; in addition to the means of propagation of seismic waves from the hypocenters of the earthquakes to the site under study (attenuation laws depending on the magnitude and distance) (McGuire, 2004; Pérez *et al.*, 2015). Thus, for the fundamental period of oscillation ( $T_1$ ) of each building within the design spectrum, the spectral acceleration defining the design seismic forces for the building is determined.

The structural system of the building (reinforced concrete, steel, masonry, etc.) and the characteristics of the seismic actions (intensity, duration, peak ground acceleration (PGA), spectral response, etc.) play a fundamental role in estimating the degree of damage that a building could have (Bojórquez *et al.*, 2017; Bhanu *et al.*, 2019; Martineau *et al.*, 2020; Pinzón *et al.*, 2020). Therefore, it will be of interest to find the ratio between the potential for damage or destructive potential of a seismic action due to its characteristics with the maximum mezzanine distortion,  $\theta_{\max}$ , that can occur in the building. This can be useful for selecting the seismic actions with the greatest potential for damage when you have a set of accelerograms. For example, in a seismic directionality analysis in buildings, where 360 seismic actions are used, obtained from the vector combination by rotating the two horizontal components of a seismic register from  $1^\circ$  to  $360^\circ$  (Vargas *et al.*, 2018; Pinzón *et al.*, 2019).

In this research, a new index ( $\text{DPIS}_{\text{SaT}_1\text{-I}_A\text{-}\Delta\text{I}_A}$ ) is developed to define the probable damage potential of an earthquake; considering in this indicator, its Arias intensity ( $I_A$ ), its significant duration ( $\Delta_{I_A}$ ) and the spectral acceleration for the fundamental period of the building ( $\text{Sa}_{T_1}$ ). Additionally, predictive equations are developed for steel buildings, which relate this new indicator to the  $\theta_{\max}$ . For this, we analyze two 3 and 7 stories 2D steel buildings, located in the city of Oaxaca, Mexico. The seismic threat of the city is defined by 23 real seismic records in its two horizontal components (46 real accelerograms). In addition, using these actions in a spectral adjustment technique in the SeismoMatch program (Seismosoft, 2018a) 46 accelerograms compatible with the seismic threat defined by the design spectrum for the city of Oaxaca are generated by the Manual of Civil Works Design of the Federal Electricity Commission of Mexico (MDOC-CFE) (2015). The assessment of the building's seismic response is performed using incremental non-linear dynamic analysis (ADNL-IDA), where the PGA of real and compatible accelerograms is used as an incremental variable.

## BUILDINGS PROTOTYPE

3-story and 7-story steel buildings in two dimensions (2-D) are evaluated in this research. The buildings have a structural system of resistant moment frames with metal profiles type W, creep resistance ( $f_y$ ) of 50 ksi. The connections are considered fully rigid (FR prequalified connections defined in ANSI/AISC 358-16 (2016)) and with recessed supports at the bases of the columns. For the structural design, it is considered a dead load (CM) and live load (CV) for the mezzanines of  $6.5 \text{ kN/m}^2$  and  $2.5 \text{ kN/m}^2$  (CV corresponding to the office use according to the NTC-RSEE-CD (2017)) respectively; while for the roof the dead load and live load was  $5.5 \text{ kN/m}^2$  and  $1 \text{ kN/m}^2$  and (CV corresponding to the roof use according to the NTC-RSEE-

CD (2017)) respectively. To linearize the load on the frames, a tributary width of 6 m, and the weight of the structural elements was considered. The earthquake-resistant design was carried out with the ECOgcW3 program (GC Ingeniería y Diseño S.C., 2020), following the specifications of the *Load and Resistance Factor Design* (LRFD) of the ANSI/AISC 360-16 (2016) and for the modified design spectrum of the city of Oaxaca defined in the MDOC-CFE (2015) and the PRODISISv4.1 (INEEL-CFE, 2015). The conditions of soft soil and the ductility factors values ( $Q=3$ ), on-resistance ( $R_o=2$ ), redundancy ( $r=1$ ), and irregularity ( $\alpha=1$ ) were considered, based on the characteristics of the buildings.

Figure 1 shows the 2-D geometry and frame profiles of each building obtained from the structural design. From the spectral modal analysis of each frame of the buildings, it is obtained that its fundamental period,  $T_1$ , is 0.50 seconds for the 3-story and 0.86 seconds for the 7-story.

The ADNL-IDA of the frames of the buildings is carried out in the SeismoStruct program (Seismooft, 2018b). The loads considered in these analyses followed the combination of 1.0 CM +0.2 CV, based on the recommendation of PEER/ATC 72-12 (2010), to perform non-linear analyses. The beams and columns were modeled as non-linear stress-strain elements based on a uniaxial analysis of individual steel fibers. Where, the stress-strain diagram of steel was defined by a bilinear hysteresis model with hardening (Seismooft, 2018b). In this way, it is ensured that the evaluation of the non-linear behavior is carried out along the entire length of the structural elements and across their entire cross-section. Two performance criteria were used, both based on the unitary uniaxial deformation ( $\epsilon$ ) of the steel fibers; one to consider the creep ( $\epsilon_y=0.0025$ ) and another for its fracture ( $\epsilon_f=0.06$ ) (Seismooft, 2018b).

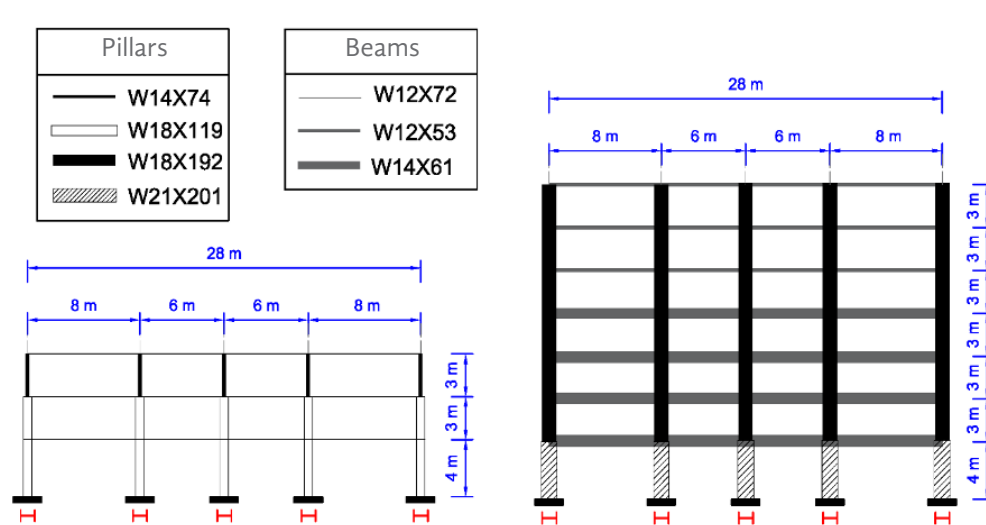


Figure 1. The geometry of the 2-D buildings used in the evaluation. Source: Own elaboration

## SEISMIC ACTIONS

This research considers as a study area the city of Oaxaca, Oaxaca, Mexico; which due to its location on the Pacific Ocean coast is subject to significant seismic activity, due to the convergences of the Cocos and North American tectonic plates (Vladimir & Pacheco, 1999). To characterize the dangerousness of this city, 23 records of real accelerations are used in its two horizontal components, East-West (E-O) and North-South (N-S) (46 real accelerograms). The seismic data were provided by the Accelerographic Network of the Institute of Engineering of the UNAM (RAII-UNAM, 2020), a product of the instrumentation and processing work of the Seismic Instrumentation Unit. The data were distributed through the Accelerographic Database System on the website: <https://aplicaciones.iingen.unam.mx/AcelerogramasRSM/>

Using a spectral adjustment technique in the SeismoMatch program (Seismosoft, 2018a) and considering as a target spectrum the modified design spectrum for the city of Oaxaca (MDOC-CFE, 2015) used in the structural design of buildings; 46 compatible accelerograms are generated. Figure 2 shows the spectra of the set of real and compatible accelerograms, in addition to the target design spectrum. The main characteristics of the set of real and compatible accelerograms are shown in Table 1; these are the register's name; epicenter distance ( $D_{Epi}$ ); Azimuth station – epicenter ( $AZ_{Est-Epi}$ ); moment magnitude ( $M_w$ ) of the earthquake recorded; total duration ( $\Delta_r$ ); *Peak ground acceleration*, PGA, the spectral acceleration for the fundamental period of the 3-story building ( $Sa_{T_1-3 \text{ story}}$ ) and 7-story ( $Sa_{T_1-7 \text{ story}}$ ); the Arias intensity ( $I_A$ ) and its respective significant duration ( $\Delta_{IA}$ ).

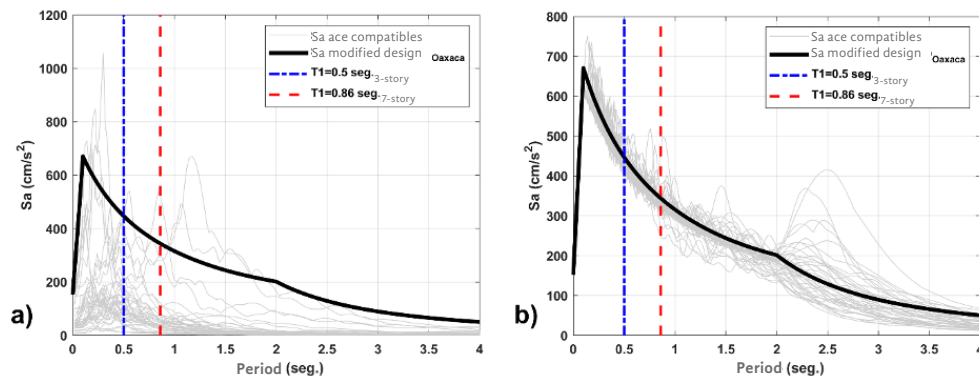


Figure 2. Response spectra of the set of a) real and b) compatible accelerograms with the modified design spectrum for the city of Oaxaca, used in the structural design of buildings. Source: Own elaboration

In this research, one of the most used indicators of the destructive potential of a seismic action in the world was used; the Arias Intensity (AI) (Arias, 1970), defined by the following equation:

$$I_A = \frac{\pi}{2g} \int_{t_i}^{t_f} (a(t))^2 \cdot dt \quad (1)$$

Where  $g$  is the acceleration due to gravity,  $t_i$  is the beginning of the accelerogram,  $t_f$  is the total duration of the accelerogram and  $a(t)$  represents the history of the acceleration time of the register component. Thus, significant duration ( $\Delta_{IA}$ ) is based on energy accumulation and is defined as the interval during which 5% to 95% Arias intensity accumulates. This interval is considered the strong phase of an earthquake (Bommer & Martínez-Pereira, 1999; Trifunac & Brady, 1975). As seen in Table 1, the 23 actual records used from the study area are varied in duration (in a range of 9.9 seconds to 229.99 seconds) and with significant destructive potential (with a moment magnitude ( $M_w$ ) greater than  $5.3^\circ$  up to  $8.2^\circ$  and peak ground acceleration, greater than  $10 \text{ cm/s}^2$  up to  $370.34 \text{ cm/s}^2$ ). In this way, we have an adequate characterization of the seismic threat to the city of Oaxaca.

**Table 1**  
Main characteristics of the set of accelerograms used in ADNL-IDA

#	Recording (RAII-UNAM, 2020)	$D_{Epi}$ (km)	$AZ_{Epi}$ (°)	Mw	$\Delta_T$ (seg.)	Comp.	Real Accelerogram Spectra						Real Accelerogram Spectra			
							PGA (cm/s <sup>2</sup> )	$Sa_{T1-3}$ Story (cm/s <sup>2</sup> )	$Sa_{T1-7}$ Story (cm/s <sup>2</sup> )	$I_A$ (cm/s)	$\Delta I_A$ (seg.)	PGA (cm/s <sup>2</sup> )	$Sa_{T1-3}$ Story (cm/s <sup>2</sup> )	$Sa_{T1-7}$ Story (cm/s <sup>2</sup> )	$I_A$ (cm/s)	$\Delta I_A$ (seg.)
1	OAXM7811.292	149.78	184.56	5.3	9.9	E-O	37.84	41.97	9.84	0.0171	7.36	228.23	501.56	352.86	0.9604	8.76
						N-S	57.22	46.03	10.43	0.0217	7.16	275.48	421.58	470.37	0.7189	7.64
2	OAXM7811.291	120.44	178.54	7.8	14.94	E-O	146.91	101.38	52.45	0.2325	7.61	265.83	430.67	313.59	0.9936	11.72
						N-S	217.10	190.93	78.18	0.5436	7.74	219.04	482.14	356.73	0.9227	11.53
3	OAXM7207.081	143.92	200.51	6.1	18.12	E-O	40.67	13.03	5.54	0.0074	7.14	239.64	421.78	316.42	0.7388	10.00
						N-S	36.12	12.29	9.67	0.0071	9.32	255.68	415.14	327.38	0.8976	13.73
4	OAXM8010.241	197.08	302.54	7	33.9	E-O	162.61	34.55	14.10	0.0991	15.36	275.23	445.79	329.72	0.9320	18.74
						N-S	116.35	53.31	22.73	0.0917	18.46	259.23	413.13	320.93	1.3081	19.63
5	OAXM7308.281	137.22	11.93	6.8	40.41	E-O	163.58	176.97	57.48	0.5821	14.58	235.83	416.71	334.32	1.3739	20.35
						N-S	199.03	336.87	86.00	0.8449	16.15	248.80	416.66	322.93	1.8062	23.76
6	OAXM9802.031	159.28	166.44	6.4	52.63	E-O	71.02	74.91	51.78	0.0451	27.48	231.85	453.49	322.24	1.2704	21.59
						N-S	45.69	65.09	29.95	0.0414	26.15	268.34	423.17	320.87	1.6259	30.36
7	OAXM0401.132	129.92	200.79	5.7	61	E-O	56.22	172.01	59.10	0.0340	11.60	287.87	428.87	330.68	0.9130	23.28
						N-S	42.96	137.50	38.61	0.0295	14.14	230.97	460.10	343.66	1.0672	19.77
8	OAXM0408.181	191.59	119.06	5.7	71	E-O	49.31	122.89	48.63	0.0446	14.37	252.89	412.76	379.62	1.3395	23.13
						N-S	38.92	155.38	52.61	0.0330	16.43	245.46	404.47	302.64	0.9696	17.21
9	OAXM0408.071	137.04	91.34	5.9	80	E-O	45.22	120.12	37.98	0.0581	22.73	298.88	499.86	324.33	1.4640	24.22
						N-S	48.14	122.19	42.53	0.0468	29.58	243.06	461.39	348.30	1.0282	19.43
10	OAXM0206.072	133.13	191.65	5.6	84	E-O	29.96	87.97	39.01	0.0171	18.97	243.31	463.52	327.62	1.0590	20.72
						N-S	26.41	85.60	38.60	0.0149	22.04	220.13	421.45	349.57	1.4753	40.24
11	OXT00408.071	139.72	91.10	5.9	104	E-O	34.07	69.25	69.14	0.0277	30.77	255.11	410.67	324.54	1.2239	31.50
						N-S	28.22	49.39	66.63	0.0276	24.73	240.91	415.26	330.65	1.1384	27.92
12	OXPC1405.211	175.81	87.63	5.8	112	E-O	10.07	26.07	5.05	0.0017	22.97	228.56	447.90	323.37	1.9400	53.53
						N-S	12.70	34.77	10.58	0.0017	25.85	271.80	424.68	326.17	1.5316	37.99
13	OAXM9909.301	130.26	194.80	7.6	112.8	E-O	370.34	355.88	108.99	3.2614	19.49	239.52	466.78	333.01	2.2472	32.31
						N-S	352.60	342.93	74.39	2.8233	17.95	203.13	403.50	323.31	1.4493	23.65
14	OXCUI511.281	8.22	263.18	4.6	122.89	E-O	16.33	54.99	39.41	0.0103	27.19	294.21	414.53	367.74	1.5430	34.85
						N-S	20.40	56.41	40.31	0.0129	20.89	235.00	429.20	327.17	1.4667	32.52
15	OXPC1802.161	165.76	236.20	7.2	122.89	E-O	16.33	54.99	39.41	0.0103	27.19	294.21	414.53	367.74	1.5430	34.85
						N-S	20.40	56.41	40.31	0.0129	20.89	235.00	429.20	327.17	1.4667	32.52
16	OXCUI807.191	138.50	302.82	5.9	156.99	E-O	32.62	73.35	77.22	0.0257	27.57	220.33	438.27	248.40	0.7870	24.76
						N-S	34.84	61.87	106.54	0.0300	25.34	252.89	449.81	328.02	1.0362	28.38
17	OXPC1407.291	136.59	57.95	6.4	167	E-O	40.50	127.07	20.98	0.0490	33.10	222.43	482.97	326.71	1.6993	49.76
						N-S	48.47	103.92	26.01	0.0454	36.50	223.71	427.58	342.99	1.3203	42.62
18	OAXM1709.232	179.69	111.06	6.1	178.99	E-O	43.85	129.16	58.32	0.0358	20.65	300.12	416.80	318.86	1.2643	24.51
						N-S	43.85	129.16	58.32	0.0358	20.65	300.12	416.80	318.86	1.2643	24.51
19	OXAE0802.121	249.37	110.90	6.6	181.13	E-O	38.44	110.10	40.32	0.0367	44.53	227.25	502.84	329.83	1.2192	34.85
						N-S	30.14	96.24	54.18	0.0356	23.20	260.99	436.03	314.38	1.5198	38.56
20	OAXM1102.251	175.51	65.57	6	195.99	E-O	35.60	71.98	34.85	0.0262	39.11	255.41	426.60	356.12	1.3228	39.27
						N-S	36.77	101.86	27.48	0.0314	37.92	248.89	431.52	338.86	1.0816	37.89
21	OAXM1407.291	134.37	59.12	6.4	207	E-O	87.49	224.53	122.46	0.2253	29.34	219.84	410.98	274.00	0.9965	28.23
						N-S	98.23	415.33	104.25	0.2912	27.56	220.78	437.41	344.15	1.5029	37.70
22	OXCUI802.161	166.47	236.48	7.2	225.99	E-O	86.34	207.81	295.29	0.2832	28.41	293.95	416.20	313.73	1.5261	36.46
						N-S	100.74	202.89	523.54	0.3539	31.14	235.97	420.58	309.17	1.6972	40.91
23	OXPC1709.081	378.59	131.90	8.2	229.99	E-O	173.63	453.84	281.86	1.0618	39.50	233.15	494.08	334.82	1.7265	50.20
						N-S	143.38	391.97	315.68	1.0709	38.55	247.15	498.72	334.57	2.2974	48.38

Source: Own elaboration

### INCREMENTAL NONLINEAR DYNAMIC ANALYSIS

This section shows the evaluation of the seismic response of the buildings, obtaining as an output variable the maximum mezzanine distortion ( $\theta_{max}$ ). For this, incremental non-linear dynamic analyses (ADNL-IDA) are carried out, considering the Peak ground acceleration (PGA) of the set of real and incrementally compatible accelerograms until the buildings collapse. Figures 3 and 4 show the results obtained from the  $\theta_{max}$  ratio with the Arias intensity ( $I_A$ ) of each accelerogram and its respective spectral acceleration for the building period ( $Sa_{T1}$ ). It can be seen in Figures 3 and 4 that the results of the analysis of the buildings for the set of real accelerograms present a greater dispersion compared to the results for the set of compatible accelerograms;

this is due to the randomness that the real seismic actions present since they do not have a spectral adjustment (see Figure 2).

Table 2 shows the correlations between  $\theta_{max}$  with  $I_A$  and  $Sa_{T1}$ . It is observed that by using compatible accelerograms in the analyses, it is possible to obtain a better correlation between the output response ( $\theta_{max}$  which represents the damage in the building) with the characteristics of the seismic actions used ( $I_A$  and  $Sa_{T1}$ ). The  $Sa_{T1}$  has the best correlation for both 3 and 7-story buildings, as well as for real and compatible accelerograms.

**Table 2**

Correlation between  $\theta_{max} - I_A - Sa_{T1}$ , obtained from the results of the ADNL-IDA analyses

Building	Real accelerograms			Compatible accelerograms		
	Variable	$Sa_{T1}$	$I_A$	Variable	$Sa_{T1}$	$I_A$
3 story	$\theta_{max}$	0.72	0.40	$\theta_{max}$	0.89	0.85
7 story	$\theta_{max}$	0.65	0.39	$\theta_{max}$	0.90	0.86

Source: Own elaboration

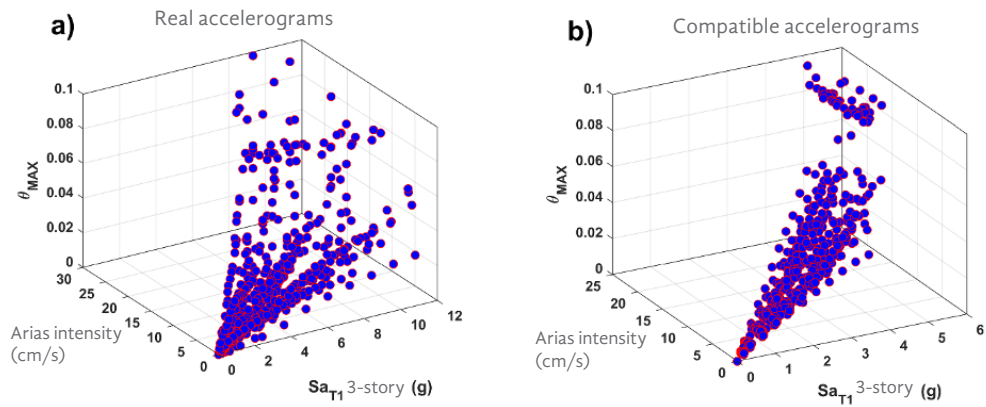


Figure 3.  $\theta_{max} - I_A - Sa_{T1}$  ratio obtained from the ADNL-IDA for the 3-story building and the a) Real and b) Compatible accelerograms. Source: Own elaboration

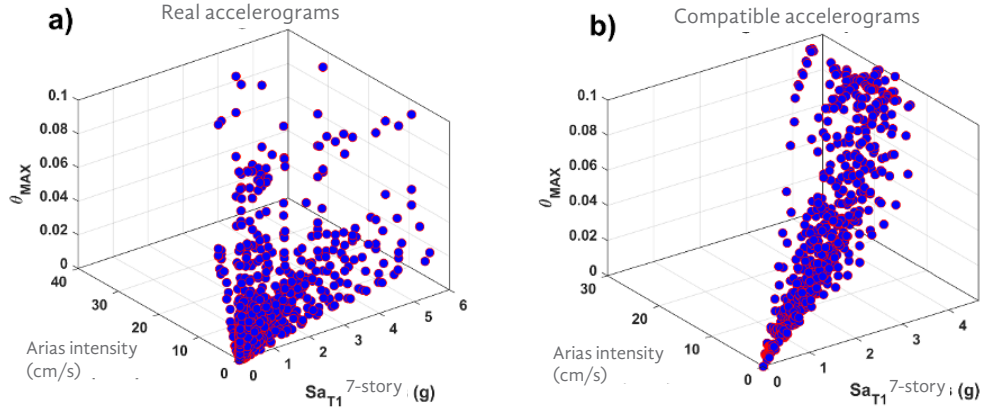


Figure 4.  $\theta_{max} - I_A - Sa_{T1}$  ratio obtained from the ADNL-IDA for the 7-story building and for the a) Real and b) Compatible accelerograms. Source: Own elaboration

### NEW DAMAGE POTENTIAL INDEX OF A SEISMIC ACTION

The correlations obtained between  $\theta_{max}$  with  $I_A$  and  $Sa_{T1}$  can be considered acceptable (especially when compatible accelerograms are used and if we consider  $Sa_{T1}$ ) to predict the destructive potential that a seismic action could have to cause damage to the structure. However, it is considered that these can be improved if we raise a new damage potential index (DPI) of a seismic action according to several of its characteristics. For this research, a DPI based on three characteristics is presented: 1)  $Sa_{T1}$ ; 2)  $I_A$  and 3)  $\Delta_{IA}$ . The following equation shows the proposed  $DPI_{SaT1-IA-\Delta IA}$ :

$$IPD_{SaT1-IA-\Delta IA} = Sa_{T1}^\alpha \left( \frac{I_A}{\Delta_{IA}} \right)^\beta \tag{2}$$

Where  $\alpha$  and  $\beta$  are calibration factors. In this DPI, it is observed it has two parts; the first is the influence of  $Sa_{T1}^\alpha$ , which as it was obtained in the ADNL-IDA of the buildings was the variable with the best correlation with the  $\theta_{max}$ . The second term  $(I_A/\Delta_{IA})^\beta$  considers the influence of the energy accumulation of the seismic action for a significant duration.

The second term of equation (2) allows the condition that a short-duration seismic action represents a greater destructive potential than a long-duration seismic action to be evaluated in the proposed index if both have the same Arias intensity (accumulated energy). For the development of this new DPI, a calibration process was carried out with the results of the buildings' ADNL-IDA, to determine the optimal values of  $\alpha$  and  $\beta$ . The values obtained for each case are presented in Table 3.

**Table 3**

Values  $\alpha$  and  $\beta$  were used in the calibration of the  $DPI_{SaT1-IA-\Delta IA}$

Building	Real accelerograms		Compatible accelerograms	
	$\alpha$	$\beta$	$\alpha$	$\beta$
3 story	0.80	0.10	1.35	0.10
7 story	0.75	0.15	1.55	0.10

Fuente: Elaboración propia

Figures 5 and 6 show the  $\theta_{max}$  ratio with the  $DPIs_{SaT1-IA-\Delta IA}$  for the 3 and 7-story buildings and the set of real and compatible accelerograms. Table 4 shows the correlations of  $\theta_{max}$  with the  $DPIs_{SaT1-IA-\Delta IA}$  of each case. Note that these increased for both buildings and both sets of accelerograms if we compare them with the correlations obtained in Table 2 for  $\theta_{max} - I_A - Sa_{T1}$ .

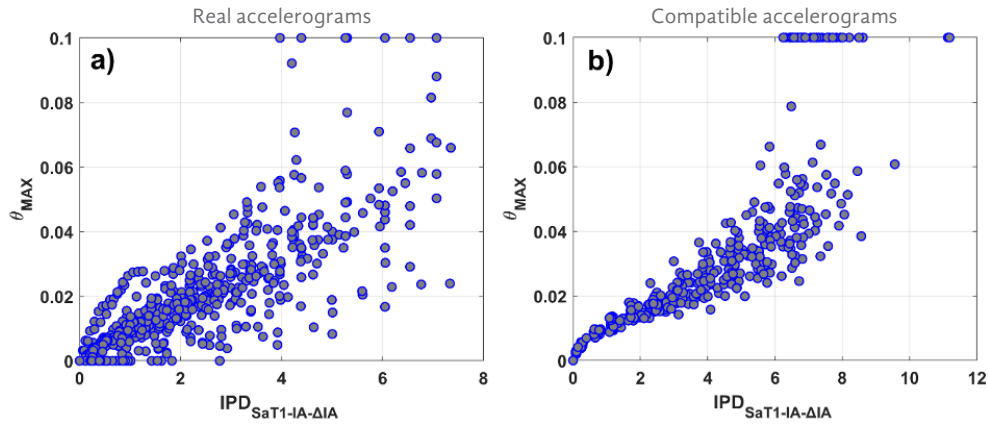


Figure 5.  $\theta_{max} - DPIs_{SaT1-IA-\Delta IA}$  ratio for the 3-story building and the a) real accelerograms and b) compatible accelerograms. Source: Own elaboration

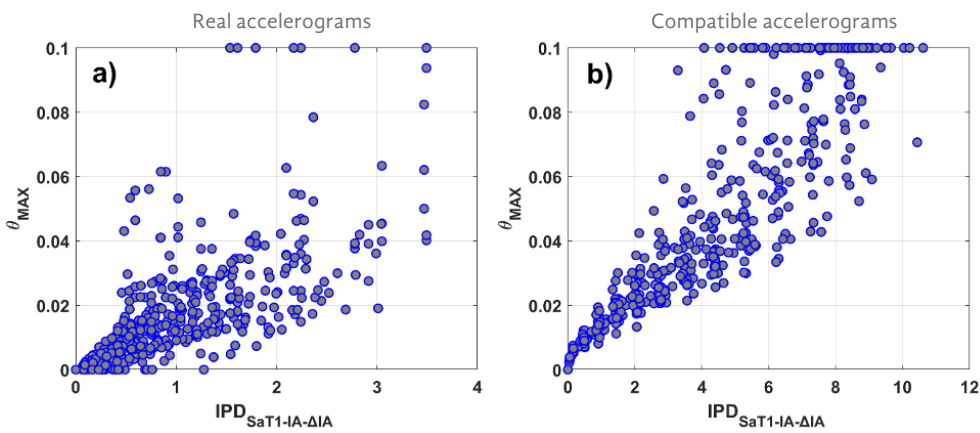


Figure 6.  $\theta_{max} - DPIs_{SaT1-IA-\Delta IA}$  ratio for the 7-story building and for the a) real accelerograms and b) compatible accelerograms. Source: Own elaboration

**Table 4**  
Correlation between  $\theta_{max} - DPIs_{SaT1-IA-\Delta IA}$

Building	Real accelerograms		Compatible accelerograms	
	Variable	IPD <sub>SaT1-IA-ΔIA</sub>	Variable	IPD <sub>SaT1-IA-ΔIA</sub>
3 story	$\theta_{max}$	0.72	$\theta_{max}$	0.89
7 story	$\theta_{max}$	0.65	$\theta_{max}$	0.90

Source: Own elaboration

PREDICTIVE EQUATIONS

Because the proposed  $DPIs_{SaT1-IA-\Delta I}$  may be an alternative for measuring the destructive or damage potential likely to be caused by a seismic action. This last section presents a proposal of predictive equations to relate this new index with the output variable that determines the damage in a building, the  $\theta_{max}$ . The best settings were presented for analyses of the 3 and 7-story buildings with the set of compatible accelerograms. While with the set of real accelerograms, the adjustments were not shown to be adequate to be considered predictive. Figure 7 shows the adjustments and predictive equations for the 3-story buildings (Ec. 3) and 7-story (Ec. 4) with compatible accelerograms. A suitable fit was achieved for these cases, being useful in future steel building investigations.

$$\theta_{max} = 0.0063(IPD_{SaT1-IA-\Delta IA} + 0.0023), \text{ for 3-story buildings} \tag{3}$$

$$\theta_{max} = 0.0063(IPD_{SaT1-IA-\Delta IA} + 0.0023), \text{ for 7-story buildings} \tag{4}$$

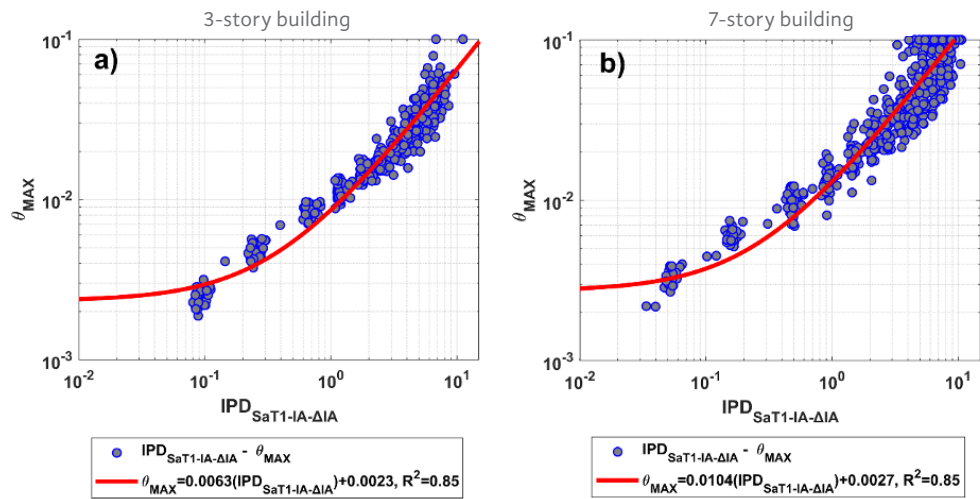


Figure 7. Linear equation adjustment for  $\theta_{max} - DPIs_{SaT1-IA-\Delta IA}$  ratio in a) 3-story and b) 7-story buildings for compatible accelerograms. Source: own elaboration

## CONCLUSIONS

This research aimed to present a new earthquake potential index, referred to in this article as the  $DPI_{SaT_1-I_A-\Delta I_A}$ . Name given as a function of three characteristics of the symbolic actions: 1) the spectral acceleration for the fundamental period of the building ( $Sa_{T_1}$ ) the Arias intensity ( $I_A$ ), and 3) its respective significant duration ( $\Delta I_A$ ). Predictive equations were also shown to determine the maximum mezzanine distortion ( $\theta_{max}$ ) based on this new index. For this, incremental non-linear dynamic analysis (ADNL-IDA) was performed on 2D 3-story and 7-story steel buildings and for real and adjusted seismic actions to the design spectrum of Oaxaca city. Several relevant conclusions obtained are presented below: i) The values obtained of  $\theta_{max}$  for both buildings show a lower dispersion for the set of compatible accelerograms compared to those obtained for the actual accelerograms. This is to be expected since the real accelerograms are very varied in their spectral accelerations, and with spectral adjustment, these become similar and of the order of the ordinates of the design spectrum. ii) The correlation of  $\theta_{max}$  with  $Sa_{T_1}$  e  $I_A$  of seismic actions is good in the analyses with the set of compatible accelerograms. The  $DPI_{SaT_1-I_A-\Delta I_A}$  proposed achieves a better correlation with  $\theta_{max}$  compared to using only  $Sa_{T_1}$  or  $I_A$  separately; both for the set of real and compatible accelerograms, as well as for the two buildings studied. iii) The presented predictive equations correctly relate the new damage potential index to  $\theta_{max}$  for seismic actions compatible with particular cases of low and medium-height steel buildings.

From the above, it is concluded that  $DPI_{SaT_1-I_A-\Delta I_A}$  represents a good alternative to measure the destructive potential of seismic actions. So, if you have a wide set of accelerograms that you want to use, you can select only seismic actions that based on their  $DPI_{SaT_1-I_A-\Delta I_A}$  represent a greater damage potential to the structure you want to analyze. Moreover, the proposed equations allow us to obtain a rapid estimate of the expected value in the  $\theta_{max}$  for each seismic action in buildings of the typologies studied here.

## REFERENCES

- ANSI/AISC 358-16.** (2016). “Prequalified connections for special and intermediate steel moment frames for seismic applications”, *American National Standard and American Institute of Steel Construction*, EUA. Disponible en: <https://www.aisc.org/products/publication/standards/prequalified-connections-ansiaisc-358-16-with-ansiaisc-358s1-18-and-ansiaisc-358s2-20/>
- ANSI/AISC 360-16.** (2016). *Specification for Structural Steel Buildings*. American Institute of Steel Construction. Chicago, Illinois 60601-6204, EUA. <https://www.aisc.org/products/publication/standards/specification-for-structural-steel-buildings-ansiaisc-360-162/>
- Arias A.** (1970). *A measure of earthquake intensity*. Cambridge, MA: MIT Press; pp. 438–83.
- ASCE/SEI 7-16.** (2016). *Minimum Design Loads for Buildings and Other Structures*, *ASCE/SEI 7-16*, *American Society of Civil Engineers/Structural Engineering Institute*, Reston, Virginia, EUA. <https://ascelibrary.org/doi/book/10.1061/9780784408094>
- Barbat, A. H., Carreño, M. L., Pujades, L. G. y Lantada, N., Cardona, O. D. & Marulanda, M. C.** (2010). “Seismic vulnerability and risk evaluation methods for urban areas. A review with application to a pilot area”. *Structure and Infrastructure Engineering*, 6(1-2), 17–38. <https://doi.org/10.1080/15732470802663763>
- Bhanu, V., Chandramohan, R., y Sullivan, T. J.** (2019). “Investigating the influence of ground motion duration on the dynamic deformation capacity of reinforced concrete framed structures”. *Pacific Conference on Earthquake Engineering and Annual NZSEE*, 1–8. <http://hdl.handle.net/10092/17414>
- Bojórquez E., Chávez R., Reyes-Salazar A., Ruiz S. E. y Bojórquez J.** (2017). A new ground motion intensity measure IB. *Soil Dynam Earthq Eng*, 99(1), 97–107. <https://doi.org/10.1016/j.soildyn.2017.05.011>
- Bommer J.J. y Martínez-Pereira A.** (1999). The effective duration of earthquake strong motion. *J Earthq Eng*. 3(1), 127–72. <https://doi.org/10.1080/13632469909350343>
- CEN.** (2019). “Eurocode 8: Design of structures for earthquake resistance. Part 1: general rules, seismic actions, and rules for buildings”. EN 1998–1:2004. *Comité Européen de Normalisation, Brussels*. (p. 231) <https://www.wiley.com/en-gb/Design+of+Steel+Structures+for+Buildings+in+Seismic+Areas:+Eurocode+8:+Design+of+Structures+for+Earthquake+Resistance+Part+1:+General+Rules,+Seismic+Action+and+Rules+for+Buildings-p-9783433030103>
- Díaz S.A., Pujades L.G., Barbat A.H., Hidalgo-Leiva D.A y Vargas Y.F.** (2018). Capacity, damage and fragility models for Steel buildings. A probabilistic

- approach. *Bulletin of Earthquake Engineering*, 16(1), 1209-1243. <https://doi.org/10.1007/s10518-017-0237-0>
- GC Ingeniería y Diseño S.C.** (2020). Software Estructuras de Concreto Reforzado, Gerardo Corona. *ECOgcW3*. <https://www.gcingeneria.com/programas/ecogcw3.html>
- INEEL-CFE.** (2015). Software PRODISISv4.1. *Instituto Nacional de Electricidad y Energías Limpias. Comisión Federal de Electricidad*. México.
- Kazantzi, A. K., Vamvatsikos, D., y Lignos, D. G.** (2014). Seismic performance of a steel moment-resisting frame subject to strength and ductility uncertainty. *Engineering Structures*, 78(1), 69–77. <https://doi.org/10.1016/j.engstruct.2014.06.044>
- Kostinakis, K. G., Athanatopoulou, A. M., y Morfidis, K. E.** (2014). Correlation between ground motion intensity measures and seismic damage of 3D R/C buildings. *Engineering Structures*, 82(1), 151–167. <https://doi.org/10.1016/j.engstruct.2014.10.035>
- Martineau, M., Lopez, A. F., y Vielma, J. C.** (2020). Effect of Earthquake Ground Motion Duration on the Seismic Response of a Low-Rise RC Building. *Advances in Civil Engineering*, 8891282. <https://doi.org/10.1155/2020/8891282>
- McGuire R. K.** (2004). Seismic hazard and risk analysis. *Institute Earthquake Engineering Research*. Oakland, CA, pp. 240.
- MDOC-CFE.** (2015). Manual de diseño de obras civiles. Diseño por sismos. *Comisión Nacional de Electricidad (CFE)*. México, pp. 745. <https://www.gob.mx/ineel/articulos/manual-de-diseno-de-obras-civiles-diseno-por-sismo-logro-de-la-ingenieria-de-mexico>
- Newmark N. M. y Hall W. J.** (1982). Earthquake spectra and design. *Earthquake Engineering Research Institute*. Berkeley, California, USA, p.103.
- NTC-RSEE-CM.** (2017). Norma Técnica Complementaria para la Revisión de la Seguridad Estructural de las Edificaciones de la Ciudad de México. *Gaceta Oficial del Gobierno de México*, p. 712. [https://www.google.com/url?sa=t&source=web&rct=j&url=https://www.smig.org.mx/archivos/NTC2017/normas-tecnicas-complementarias-reglamento-construcciones-cdmx-2017.pdf&ved=2ahUKEwikrNf\\_i6nxAhXtQjABHfaeD3MQFjAAegQIBBAC&usg=AOvVawocGCv1wQNw4fqY2islepqa](https://www.google.com/url?sa=t&source=web&rct=j&url=https://www.smig.org.mx/archivos/NTC2017/normas-tecnicas-complementarias-reglamento-construcciones-cdmx-2017.pdf&ved=2ahUKEwikrNf_i6nxAhXtQjABHfaeD3MQFjAAegQIBBAC&usg=AOvVawocGCv1wQNw4fqY2islepqa)
- PEER/ATC 72-1.** (2010). Modeling and acceptance criteria for seismic design and analysis of tall buildings. *Applied Technology Council and Pacific Earthquake Engineering Research Center*, pp. 242. Disponible en: [https://store.atcouncil.org/index.php?dispatch=products.view&product\\_id=242](https://store.atcouncil.org/index.php?dispatch=products.view&product_id=242)
- Pérez, R. L. E., Mena, H. U., Tena, C. A., y Mena, S. E.** (2015). Espectros de diseño sísmico para la nueva versión del manual de diseño de obras civiles de CFE. *XX Congreso Nacional de Ingeniería Sísmica. Acapulco, Guerrero*. Disponible en: [https://www.researchgate.net/publication/316919665\\_](https://www.researchgate.net/publication/316919665_)

Espectros\_de\_diseno\_sismico\_para\_la\_nueva\_version\_del\_Manual\_de\_Diseño\_de\_Obras\_Civiles\_de\_CFE

- Perrault**, M. y Guéguen, P. (2015). Correlation between ground motion and building response using Californian earthquake records. *Earthquake Spectra. Earthquake Engineering Research Institute*, 31(4), 2027. <https://doi.org/10.1193/062413EQS168M>
- Pinzón**, L. A., Vargas-Alzate, Y. F., Pujades, L. G. y Diaz, S. A. (2020). A drift-correlated ground motion intensity measure: Application to steel frame buildings. *Soil Dynamics and Earthquake Engineering*. 132(1), 106096. <https://doi.org/10.1016/j.soildyn.2020.106096>
- Pinzón**, L. A., Díaz, S. A., Pujades, L. G. y Vargas, Y. F. (2019). An Efficient Method for Considering the Directionality Effect of Earthquakes on Structures. *Journal of Earthquake Engineering. Article 25(9)*, 1679-1708. <https://doi.org/10.1080/13632469.2019.1597783>
- RAII-UNAM**. (2020). *Red Acelerográfica del Instituto de Ingeniería de la UNAM*. <https://aplicaciones.iingen.unam.mx/AcelerogramasRSM/Inicio.aspx>
- Seismosoft**. (2018a). SeismoMatch. Earthquake Software for Response Spectrum Matching. Italia. Disponible en: <https://seismosoft.com/products/seismomatch/>
- Seismosoft**. (2018b). SeismoStruct. *Civil Engineering Software for Structural Assessment y Structural Retrofitting*. Italia. <https://seismosoft.com/products/seismostruct/>
- Trifunac**, M. D. y Brady, A. G. (1975). A study on the duration of strong earthquake ground motion. *Bull Seismol Soc Am*, 65(1), 581–626. <https://pubs.geoscienceworld.org/ssa/bssa/article-abstract/65/3/581/101795/A-study-on-the-duration-of-strong-earthquake?redirectedFrom=fulltext>
- Vamvatsikos** D. (2014). Seismic performance uncertainty estimation via IDA with progressive accelerogram-wise Latin Hypercube Sampling. *Journal of Structural Engineering*. 140(8), 1-10. [https://doi.org/10.1061/\(ASCE\)ST.1943-541X.0001030](https://doi.org/10.1061/(ASCE)ST.1943-541X.0001030)
- Vamvatsikos** D. y Cornell C.A. (2002). Incremental dynamic analysis. *Earthquake Engineering and Structural Dynamics*. 31(3), 491-514. <https://doi.org/10.1002/eqe.141>
- Vargas** Y.F., Pujades L.G., Barbat A.H., Hurtado E., Diaz S.A. y Hidalgo-Leiva D. A. (2018). Probabilistic seismic damage assessment of reinforced concrete buildings considering directionality effects. *Structure and Infrastructure Engineering*, 14(6), 817-829. <https://doi.org/10.1080/15732479.2017.1385089>
- Vladimir** K. & Pacheco J.F. (1999). *Cien años de sismicidad en México. Poster del Instituto de Geofísica*, Universidad Nacional Autónoma de México UNAM. <http://usuarios.geofisica.unam.mx/vladimir/sismos/100a%F1os.html>